DOI: 10.26599/FSHW.2025.9250573

Contents lists available at SciOpen

Food Science and Human Wellness

journal homepage: https://www.sciopen.com/journal/2097-0765

China Food Publishing Co.

Mesona chinensis Benth polysaccharide improves intestinal barrier function in dextran sodium sulfate-induced human Caco-2 cells and its molecular mechanisms

Fengxia He[a], Hanyu Lu[a], Xianxiang Chen[a], Junwei Zhao[b], Xiaoyan Ou[b], Jianhua Xie[a] *

[a] *State Key Laboratory of Food Science and Resources, Nanchang University, Nanchang 330047, China*

[b] *School of Stomatology, Jiangxi Medical College, Nanchang University, Nanchang, 330006, China*

ABSTRACT: *Mesona chinensis* Benth is a traditional medicinal and edible plant commonly used in China. Previous studies have found that *Mesona chinensis* Benth polysaccharide (MBP) can exhibit anti-inflammatory and antioxidant activities, also alleviate colitis development in mice. To further investigate the effects of MBP on intestinal cell and intestinal barrier, dextran sodium sulfate (DSS)-induced inflammation models in Caco-2 cells were constructed. Our investigation results showed that DSS induced strong cytotoxicity on Caco-2 cells, while MBP intervention enhanced cell viability and alleviated cell damage through inhibiting lactate dehydrogenase (LDH) production. Moreover, DSS induced a dysregulated oxidative stress state, which can be ameliorated by MBP intervention through enhancing superoxide dismutase (SOD) activity, decreasing reactive oxygen species (ROS) content and reducing the secretion of inflammatory factors such as tumour necrosis factor-α (TNF-α) and interleukin 6 (IL-6), as well as decreasing the expression of cyclooxygenase (COX-2) protein. Additionally, MBP can ameliorate cell cycle arrest and attenuate apoptosis which was caused by DSS via the Caspase-3/Bcl-2/Bax pathway. Furthermore, MBP intervention could maintain the integrity and stability of Caco-2 monolayer cell, which was indicated by fall of fluorescent yellow permeability, rise of trans-epithelial electrical resistance (TEER) value and expression content of tight junction proteins (TJs) such as ZO-1, Occludin, and Claudin. These findings suggested that MBP may be developed as an intestinal protective agent, which will expand the application range and value of *Mesona chinensis* Benth.

Keywords: *Mesona chinensis* Benth polysaccharide; Intestinal injury; Caco-2 monolayer model; anti-inflammatory; antioxidant

1. Introduction

The intestinal epithelium is the largest and most important single-cell barrier, separating the lamina propria from the external environment. It serves as the first defence line of the mucosal immune system, regulating the passage of solutes and antigens [1-2]. On one hand, it allows the entry of necessary nutrients into the organism's internal circulation, on the other hand, effectively prevents the passage of foreign harmful substances, such as antigens and biotoxins. Impaired intestinal barrier function is associated with the development of ulcerative colitis (UC). Studies have shown that dysfunction of the intestinal barrier will

***Corresponding author**
jhxie@ncu.edu.cn(J. Xie)

Received 30 October 2024
Received in revised from 22 November 2024
Accepted 7 February 2025

result in invasion of the intestinal luminal antigens into lamina propria, thus it is an important factor promoting the development of intestinal inflammation. Therefore, protecting the intestinal barrier can help mitigate the progression of colitis [3-5].

Mesona chinensis Benth, also known as the *Hsian-tsao*, has a long history of use in China for both edible and medicinal purposes. In recent years, extensive research has been conducted on the functional active components and biological activities of *Mesona chinensis* Benth. Its mainly active ingredients, such as polysaccharides, flavonoids, terpenes and phenols, exhibit biological activities such as antioxidant, hypoglycemic, hypolipidemic, hypotensive, antiviral and anti-hypoxia properties. *Mesona chinensis* Benth polysaccharide (MBP), as the main ingredient of water-soluble extracts, has shown many potential activities. Previous studies found that MBP exerts protective effects *in vitro* against oxidative imbalance and inflammatory states in RAW264.7 cells and regulatory effects in L02 cells [6-7]. Furthermore, MBP has demonstrated significant anti-inflammatory effects on ulcerative colitis induced by DSS in mouse through the TLR4/MAPK/NF-κB signaling pathways, along with the regulation of intestinal microbiota [8-10].

In vivo the effect of MBP on UC was studied on mouse, which is far from human in genetic relationship. In order to comprehensively understand the underlying regulatory mechanisms of MBP on human ulcerative colitis, in this study, DSS-induced Caco-2 cell injury models were constructed to systematically investigate the protective effects of MBP for oxidative stress and cell apoptosis on intestinal cells. Caco-2 monolayer cell models can simulate the complex anatomy of the intestine and realistically reflect the damage and repair of the intestinal barrier, which is highly advantageous for the dynamic study of colitis [11-12].

2. Materials and methods

2.1 Plant materials

Mesona chinensis Benth was purchased from Ganzhou City, Jiangxi Province. Following the laboratory procedure [13-14], the powder of *Mesona chinensis* Benth was dissolved in ultrapure water and stirred at 100℃ for 2 h, then collected and immersed in 80% (*v/v*) ethanol and steeped overnight. After three rounds of deproteinization and dialysis of the leachate, the precipitated extract was lyophilized to obtain MBP. MBP has a molecular weight of 157 kDa and is composed of glucose, xylose, galactose and galacturonic acid in a molar ratio of 1.49:2.54:0.68:6.33. Additionally, the content percentages of total sugar uronic acid and protein in MBP were 39.01%, 29.30% and 27.52%, respectively. MBP has α-(1→4)-galacturonic acid backbone [6].

2.2 Establishment of cellular models

The human epithelial cell line Caco-2 cell was purchased from National Collection of Authenticated Cell Cultures, Caco-2 cells were cultured in Dulbecco's modified Eagle's medium (DMEM; Solarbio, Beijing, China) with 10% fetal bovine serum (FBS; Biological Industries, Israel). The concentrations of MBP and DSS were determined in pre-experiment. Caco-2 cells in the logarithmic growth phase were inoculated at a density of 2×10^5 cells/mL with 100 μL per well in 96-well plates and incubated for 24 h.

Following this, for MBP group, the cells were treated with different concentrations of MBP (40, 80, 160, 320 μg/mL) and further incubated for 24 h. For the negative control (NC) and model control (MC) groups, cells were incubated with normal medium for the same duration. The following day, 4% DSS was added to all groups except NC and incubated for an additional 24 h. After the medium was changed, the optical density (OD) values at 450 nm were measured using cell counting kit-8 (CCK8; Dojindo Molecular Technologies, Inc., Kumamoto, Japan) assay to calculate the cell viability rate for each group as described in the reference [15].

2.3 Extracellular LDH content and cytokine release in Caco-2 cells

The pre-treatment of cells was conducted as described in section 2.2. Subsequently, medium supernatant from each group were collected and transferred into 96-well plate. To each well of a 96-well plate, 50 μL of the LDH assay reagent (Promega, America) were added. The plate was then incubated at room temperature for 1 h. The luminescence signals were measured using a multifunctional microplate reader, and LDH concentrations for each group were calculated accordingly. Following the identical cell treatment procedure, cytokine in the medium was detected with TNF-α and IL-6 assay kits (Boster Biological Technology, Wuhan, China).

2.4 Determination of SOD activity in Caco-2 cells

Cells in the logarithmic growth phase were inoculated at a density of 2×10^5 cells/mL, with 2 mL per well in 6-well plates, and incubated for 24 h. Subsequently, MBP of different concentrations (40, 80, 160, 320 μg/mL) were added and the incubation continued for additional 24 h. Each group had three replicate wells. Following the MBP treatment, the cells were exposed to 4% DSS and incubated for another 24 h. At the end of the incubation, the cells were washed twice with PBS buffer. IP cell lysis buffer (containing 1% protease inhibitor PMSF) was added and the cells were allowed to stand on ice for 10-15 min. The lysed cells were collected by centrifugation at 4℃ and 10000 r/min for 5 min. The supernatant was collected and SOD activity was determined with SOD assay kit (Beyotime Biotechnology, Shanghai, China), following the manufacturer's instructions. The protein content of the cell supernatant was measured using a bicinchoninic acid assay (BCA; Beyotime Biotechnology, Shanghai, China) kit. The final results were expressed as units of SOD activity per milligram of protein.

2.5 Determination of apoptotic state and cell cycle of Caco-2 cells

Following the same pre-treatment as described in section 2.4, the cells were digested with trypsin (without EDTA) and collected by centrifugation, the cells were then washed 3 times with pre-cooled PBS buffer. Thereafter, 5 μl Annexin V-FITC and 10 μl PI in Annexin V-FITC/PI Apoptosis Kit (Multi Sciences, Hangzhou, China) were added sequentially to the cell suspension. The mixture was gently vortexed and then incubated for 5 min at room temperature in the dark. After incubation, the cells were analysed using a flow cytometer.

After cells were collected with the same treatment as described above, 1 mL of DNA Staining solution and 10 μl of permeabilization solution in Cell Cycle Staining Kit (Multi Sciences, Hangzhou, China) were added into each sample and thoroughly mixed, then incubated at room temperature in the dark for 30 min. Thereafter, the samples were analysed on flow cytometer to determine DNA content.

2.6 Intracellular ROS levels in Caco-2 cells

Following the same procedure as described in section 2.5, 1 mL of DMEM medium (containing 10 mmol/L DCFH-DA) was added to the cell pellet and mixed well. The cells were then incubated for 30 min avoid from light. After the incubation, the intracellular fluorescence intensity was immediately measured on flow cytometry (BD Biosciences, C6 Plus, USA) under dark conditions. The flow cytograms of each group were recorded to analyse the relative levels of ROS within the cells.

2.7 Western blotting

The methodology followed is as described in the reference [16]. Briefly, after the cells were treated according to the procedure outlined in section 2.4, they were washed 3 times with pre-cooled PBS buffer. Subsequently, IP lysis buffer (1:20) containing 1 mmol/L PMSF was added, after incubation, samples were separated by SDS-PAGE and then transferred onto a PVDF membrane. The membrane was blocked with 5% BSA and then sequentially incubated with the appropriate primary antibody and corresponding HRP-conjugated secondary antibodies. After the final incubation, the ECL substrate solution was added to the membrane, and the target protein bands were exposed in a gel imaging system, and the protein content was analysed by Quantitative One software. IP lysis buffer, PMSF, and ECL substrate solution were purchased from Beyotime Biotechnology, Inc., HRP-conjugated secondary antibodies were purchased from Cell Signaling Technology, Inc. (America).

2.8 Caco-2 monolayer cell model

The previous method was referred to and slightly modified [16-17]. Caco-2 cells in the logarithmic growth phase were seeded in 12-well transwell plates (Corning) at a cell density of 3×10^5 cells/mL. For each well, 0.5 mL of the cell suspension was added to the Apical (AP) side of the incubation chambers, while 1.5 mL of medium was added to the outer Basolate ral (BL) side. The medium was replenished every 48 h during the first week, after which it was changed daily.

2.8.1 Establishment of Caco-2 monolayer cell model

The methodology was referred to with minor modifications [18]. Prior to use, the electrodes should be submerged in 75% alcohol for 15 min and then washed with PBS and culture medium sequentially. For the measurement, the longer section of the electrode was immersed in the BL side of the chamber, while the shorter end was inserted vertically into the AP side. Once the resistance reading stabilizes, the value is recorded. TEER was monitored using a cell transmembrane resistance meter (Millicell ERS-2, Merck, America) every 2 days during the initial 2 weeks, and then the TEER value was measured daily. After 21 days of cell growth, the TEER value was stabilized at 600-800 $\Omega\bullet cm^2$ for three consecutive days indicated a

well-developed monolayer was formed. On the 22nd day, the impact of different concentrations of MBP on the reduction of cell resistance values, induced by DSS, was assessed.

2.8.2 Fluorescent yellow penetration

After cultured for 21 days, the Caco-2 monolayer cell model was treated following the procedures outlined in section 2.2. The culture medium was aspirated, and the cells were washed three times with HBSS. After the final wash, 1.5 mL HBSS was added to the AP side, and 2.6 mL HBSS was added to the BL side. The cells were equilibrated in an incubator for 30 min. Subsequently, 0.5 mL of fluorescent yellow solution at a concentration of 0.4 mg/mL was added to the equilibrated AP side. 1.5 mL HBSS was added to the BL side, and the cells were incubated for 100 min. At 20-min intervals, 100 μL of samples were aspirated from the BL side and an equal volume of HBSS was replenished. The fluorescent intensity of all samples was measured at an excitation wavelength of 492 nm using Multiskan FC microplate reader (Thermo, America). To generate a standard curve, fluorescent yellow solutions at concentrations of 0.015, 0.02, 0.04, 0.06 and 0.08 mg/mL were prepared in HBSS buffer. The absorbance values of the solutions were measured at 492 nm using a microplate reader. A standard curve was plotted with fluorescent yellow concentration on the horizontal axis and OD value on the vertical axis. The permeability of the fluorescent yellow was calculated using the following equation.

$$Papp = \frac{\mathrm{dQ}}{\mathrm{dt} \times \mathrm{A} \times \mathrm{C_0}}$$

Where Papp is the apparent permeability coefficient (cm/s), dQ/dt is the rate of fluorescent yellow transportation during the study period (mg/s), A is the effective growth area of cells (cm^2), and C_0 is the primary concentration of the fluorescent yellow (mg/mL).

2.8.3 Detection of TJs protein

Proteins were extracted from transwell plates following the procedure detailed in section 2.8 and TJs proteins (ZO-1, Occludin, Claudin) were detected using western blotting.

2.9 Statistical analysis

Data is presented as mean ± standard deviation (SD) with a minimum of three independent measurements taken for each sample. Graphs were plotted using Graphpad Prism software, and data were analysed by one-way analysis of variance (ANOVA) with IBM SPSS Statistics 21.0 to detect differences between groups. $P < 0.05$ and $P < 0.01$ indicate significant and highly significant differences, respectively.

3. Results

3.1 MBP mitigated the viability reduction of DSS-induced Caco-2 cells

Effects of four concentrations of MBP (40, 80, 160, and 320 μg/mL) on cell viability were presented in Fig. 1A. Both in NC and MC groups, the cell viability was significantly lower without MBP treated compared with the four concentrations of MBP. Specifically, in NC group, MBP at a concentration of 320 μg/mL enhanced the cell viability by 37.27%. In the MC group, DSS induced significant cell viability reduction for

cell without MBP pre-incubation, the treatment of MBP mitigated the reduction. Notably, at a concentration of 320 μg/mL, MBP significantly improved cell survival by 83.47%.

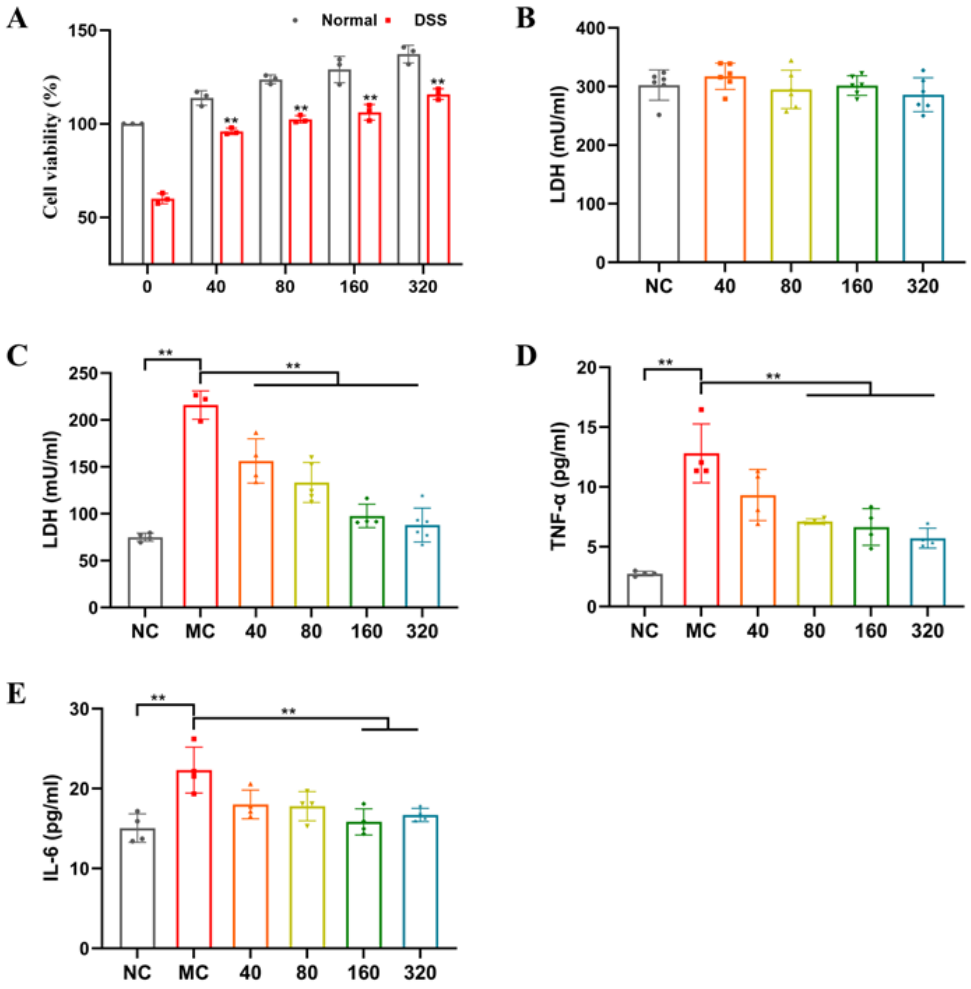

Fig. 1. Toxicity test of MBP and it exhibited protected effect in DSS-induced injury Caco-2 cells. (A) cell viability, (B, C) LDH contents, (D)TNF-α, and (E) IL-6. $P < 0.01$**, compared with MC group.

3.2 MBP reduced LDH release from DSS-induced Caco-2 cells

LDH is a stable cytoplasmic enzyme, when the cell are damaged, it will rapidly release from the cytoplasm membrane, thus it is used as a biomarker in cytotoxicity [19]. There was no significant change in the extracellular LDH content of Caco-2 cells exposed to various concentrations of MBP (Fig. 1B), indicating that MBP did not exert toxic effects on Caco-2 cells. Furthermore, Caco-2 cells treated with DSS (Fig. 1C) exhibited a significant increase in extracellular LDH content (187%) compared to the normal group. However, the addition of MBP at different concentrations significantly reduced the extracellular LDH content ($P < 0.01$) relative to MC group without MBP treatment. This reduction rates of LDH release increased with the concentrations of MBP, indicating a protective effect of MBP against DSS-induced cytotoxicity.

3.3 MBP reduced cytokine release from DSS-induced Caco-2

Polysaccharide treatment has been reported to inhibit the expression of inflammatory cytokines, including TNF-α and IL-6 [20]. After treated with DSS (Fig. 1D and E), the secretion of TNF-α and IL-6 by Caco-2 cells was significantly higher in comparison with that of the NC group ($P < 0.01$). In contrast, the

secretion of these cytokines was significantly reduced with pre-treatment of MBP at concentrations of 160, 320 μg/mL, with reduction rate of 48%-55% for TNF-α and 25%-29% for IL-6, respectively ($P < 0.01$).

3.4 MBP elevated SOD activity in DSS-induced Caco-2

SOD is a common class of antioxidant enzymes that plays a crucial role in maintaining the cellular redox homeostasis by removing excess oxygen free radicals [21]. In our study, SOD activity was significantly reduced in the MC group compared to the NC group ($P < 0.05$) (Fig. 2A). Upon incubation with high concentrations of MBP (160, 320 μg/mL), SOD activity was significantly elevated by 64% and 91%, respectively ($P < 0.01$), in comparison to the MC group. This indicates that MBP has the potential to enhance antioxidant activity in cells under oxidative stress.

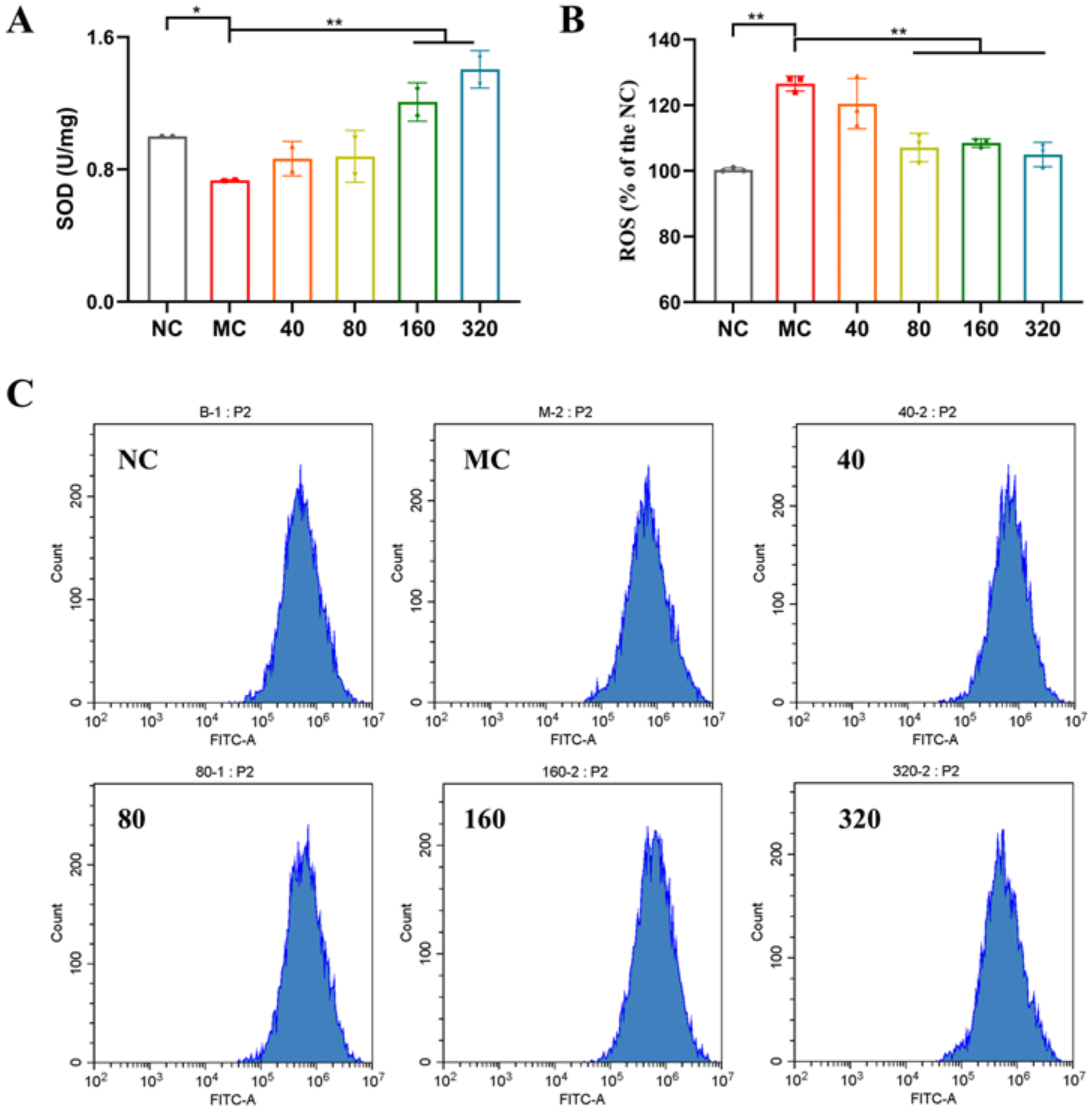

Fig. 2. Effect of MBP on the level of oxidative stress factors in DSS-induced injury Caco-2 cells. (A) SOD and (B, C) ROS. n = 3, $P < 0.05$*, $P < 0.01$**, compared with MC group.

3.5 MBP reduced ROS levels in Caco-2 cells induced by DSS

ROS are essential for normal cell physiological functions and serve as by-products of cellular metabolism. They are typically maintained in a stable dynamic equilibrium. However, an excessive accumulation of ROS can trigger cell death processes, such as apoptosis or autophagy [22-23]. Fig. 2B and C

illustrated the effect of various concentrations of MBP on ROS levels in Caco-2 cells induced with DSS. Compared to the NC group, ROS levels in the MC group were significantly higher ($P < 0.01$), indicating a disruption in oxidative state following DSS treatment. In contrast, the addition of MBP at concentrations ranging from 80 to 320 μg/mL significantly reduced intracellular ROS content, with highly significant reductions of 14%-17%.

3.6 MBP mitigated Apoptotic status in DSS-induced Caco-2 cells

Apoptosis is a highly regulated form of cell death and implicated in various pathologies. It can be triggered by an overproduction of ROS [24]. Our results indicate that DSS treatment significantly induces apoptosis, predominantly in the form of late apoptosis, as indicated by the upper right region in Fig. 3A. The apoptotic effect of DSS was substantially mitigated by treatment with different concentrations of MBP. Specifically, the apoptotic rate was reduced by 4%-50% when compared to the MC group (Fig. 3C), demonstrating a dose-dependent attenuation of apoptosis, which was similar to the trend of ROS results.

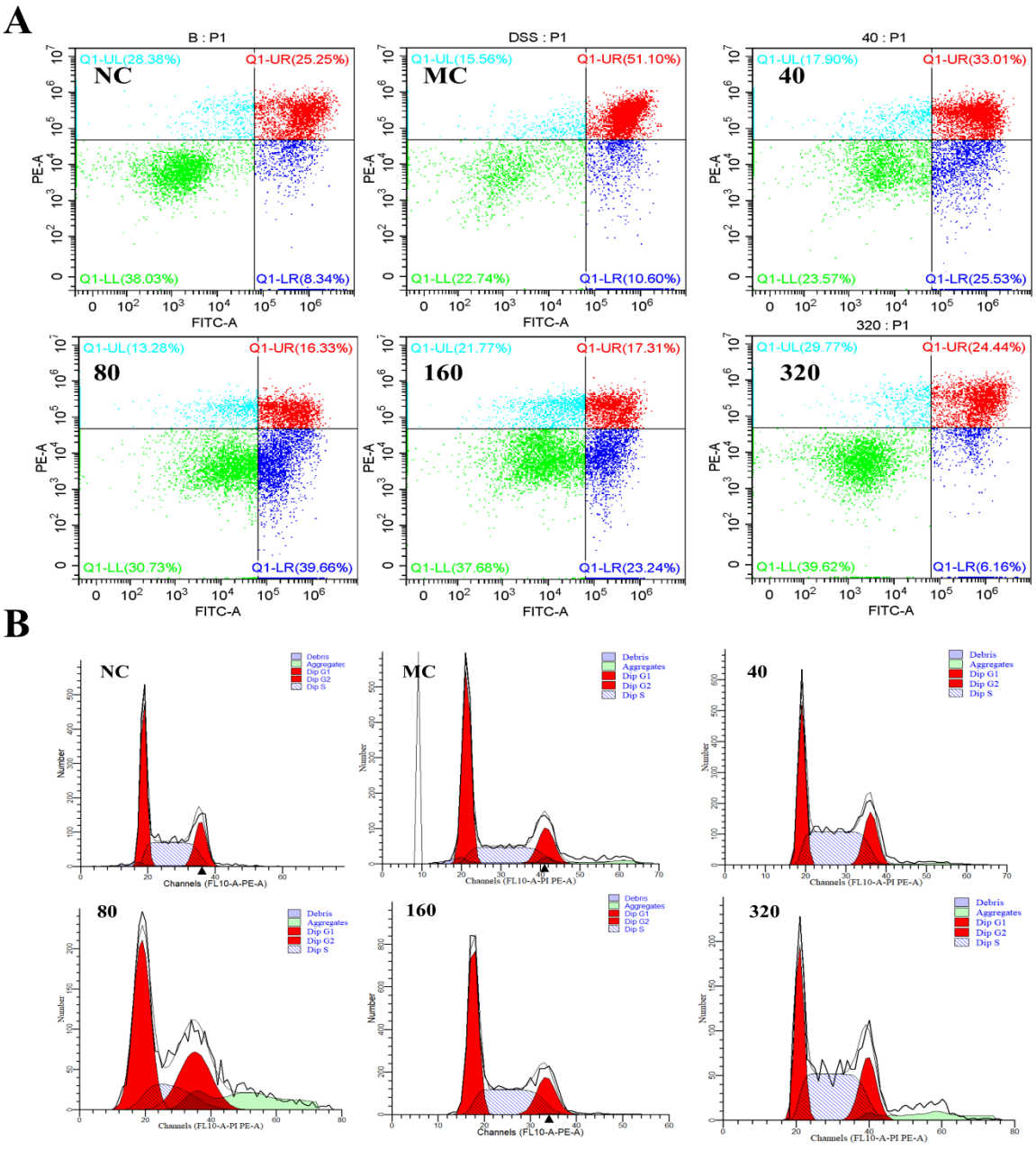

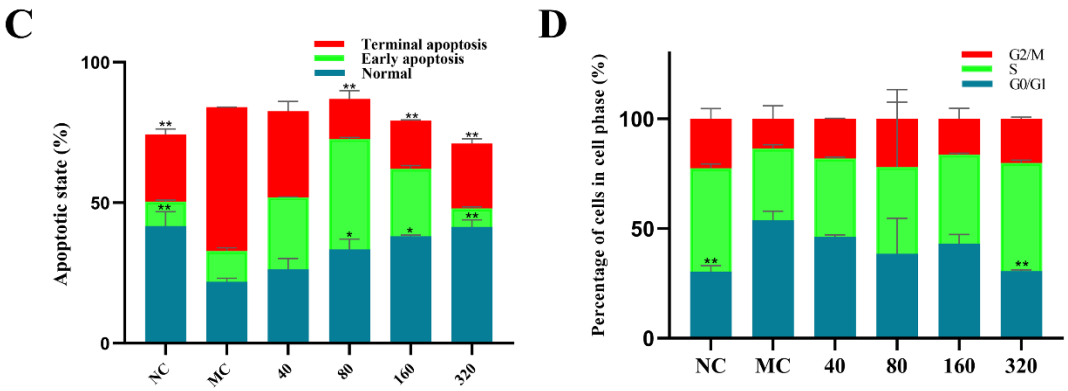

Fig. 3. Effects of MBP on the apoptosis in DSS-induced injury Caco-2 cells. (A) apoptotic state, (B) cell cycle, and (C) the ratio of each cycle. n = 3, $P < 0.01$**, compared with MC group.

3.7 MBP reduced cell ratios at G0/G1 phase in DSS-induced Caco-2 cell

The fluorescence intensity of PI directly reflects the DNA content in the cell after it binds to DNA, allowing for the differentiation of cells at various stages of the cell cycle [25-26]. In our study, compared to the NC group, where 30.41% of cells were in the G0/G1 phase, DSS treatment significantly increased this proportion to 53.74%. Concurrently, the number of cells in the S and G2/M phases decreased, indicating that DSS treatment blocked the progression of cells in the G0/G1 phase (Fig. 3B and D). Following MBP treatment, the ratio of cells in the G0/G1 phase was reduced obviously at a concentration of 320 μg/mL ($P <$ 0.01).

3.8 Expression of related proteins

The impact of MBP on the ratios of cleaved-caspase3/caspase3 and B-cell lymphoma-2 (Bcl-2)/Bax, as well as the expression of COX-2, Occludin and Claudin proteins in DSS-induced Caco-2 cells were investigated (Fig. 4). Compared to the MC group, MBP treatment significantly reduced the cleaved-caspase3/caspase3 ratio and COX-2 protein levels ($P < 0.01$) (Fig. 4A). In contrast, the Bcl-2/Bax ratio and the levels of Occludin and Claudin proteins were significantly higher in the MBP pretreatment group (Fig. 4B). MBP treatment effectively inhibited the overactivation of caspase3 and the overexpression of COX-2 protein, restored the Bcl-2/Bax ratio, and increased the expression of Occludin and Claudin, which are important for maintaining cell integrity. Compared to the MC group, MBP treatment at 320 μg/mL significantly reduced the cleaved-caspase3 to caspase3 ratio and COX protein expression ($P < 0.01$) by 61.9% and 35.4%, respectively. MBP treatment at 160 μg/mL significantly increased Bcl-2/Bax ratio and Claudin protein expression by 4.3-fold and 3.5-fold, respectively, compared to the MC group ($P < 0.01$).

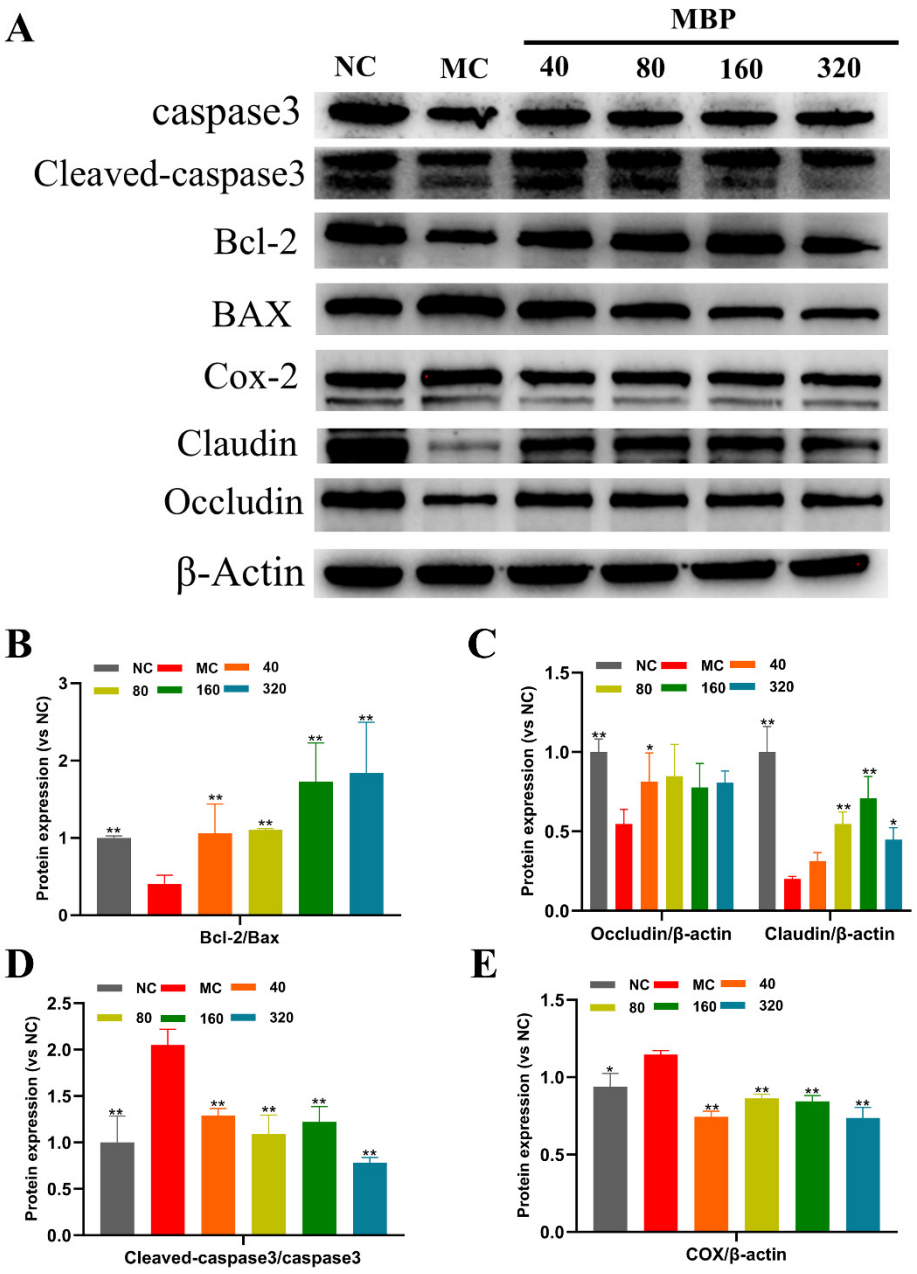

Figure 4. Effect of MBP on the protein expression of Cleaved-caspase3, caspase3, Bcl-2, Bax, COX-2, Occludin and Claudin in DSS-induced injury Caco-2 cells (A-E). n = 3, $P < 0.01$**, compared with MC group.

3.9 MBP reversed reduction of transmembrane resistance value on DSS-induced Caco-2 monolayer cell model

TEER value is a key indicator of the tightness and integrity of a monolayer cell model, with higher values suggesting tighter cell connections [27]. Our findings indicate that MBP incubation did not affect the resistance values, suggesting that it did not impair the densification of the monolayer model (Fig. 5A). In contrast, the addition of DSS led to a decrease resistance values across all groups. Notably, pre-treatment with MBP significantly reversed the decrease in resistance ($P < 0.01$).

3.10 MBP reduced fluorescent yellow permeation in DSS-induced Caco-2 cells

Our results demonstrated that the fluorescence yellow permeability of the MC group was significantly higher than that of the other groups (Fig. 5B). After 100 min of incubation of fluorescent yellow, the Papp value of MC group is substantially higher than the normal range, while the Papp values of other groups remained within the normal range (Fig. 5C). These findings indicate that the integrity of the monolayer cell model was significantly impaired after DSS treatment. However, this impairment was notably mitigated following incubation with MBP at four different concentrations ($P < 0.01$), suggesting that MBP could protect and restore the barrier function of the cell monolayer.

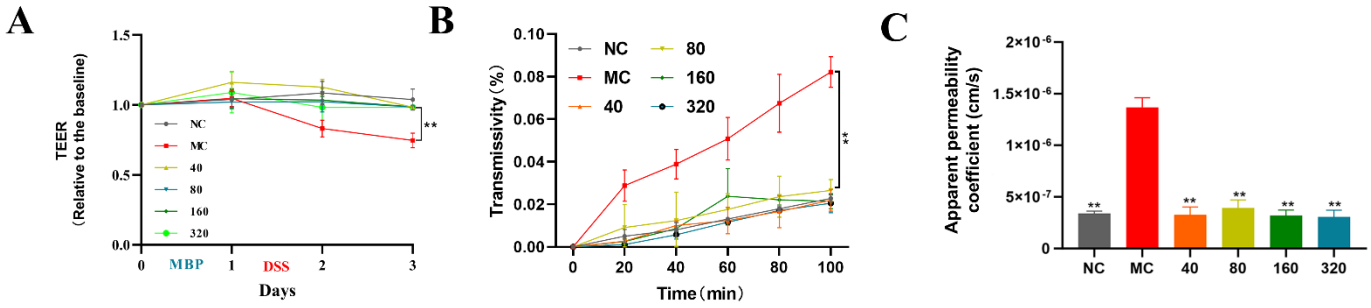

Fig. 5. Effect of MBP on Cell membrane resistance (A), fluorescent yellow permeability (B), and the Papp value of fluorescent yellow (C) at 100 min of incubation. *P < 0.01***, compared with MC group.

3.11 Expression of TJs protein

The expression of three TJs proteins (ZO-1, Occludin, Claudin) was found to be decreased after DSS injury when compared to the NC group (Fig. 6A and B). However, after pretreated with MBP, the expression of the three proteins was significantly restored. The group pretreated with MBP at a concentration of 320 μg/mL showed a significant increase in the expression of ZO-1, Occludin, and Claudin proteins by 163%, 207%, and 182%, respectively, compared to the MC group ($P < 0.01$).

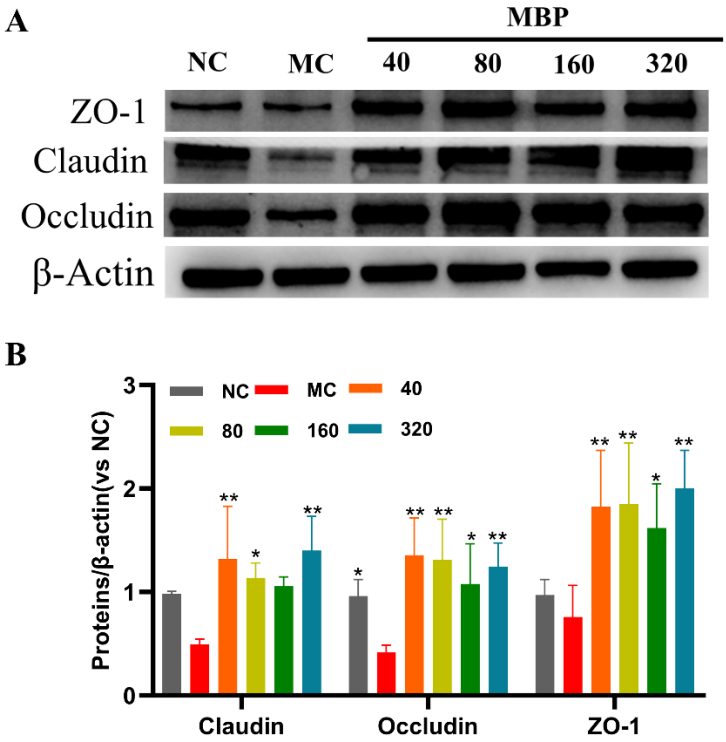

Fig. 6. Effects of MBP on DSS-induced TJs protein expression in Caco-2 monolayer cells. n = 3, *P < 0.01***, compared with the MC group.

4. Discussion

Under stressful or pathological conditions, the balance of the intestinal can be disrupted, thus forming an aerobic and inflammatory environment by producing oxygen and pro-inflammatory cytokine [28]. Intestinal oxidative and inflammatory stress can destroy the epithelial barrier, affecting nutrients digestion and absorption, which can cause a variety of harmful diseases [29]. Therefore, the stabilization of the intestine state is crucial for the maintenance of host health. Although some naturally derived polysaccharides possess antioxidant, anti-apoptotic and anti-inflammatory capacity [30-32], it is not completely clear regarding their potential mechanisms.

Caco-2 cells are usually used as a model for intestinal epithelial cells, which can mimic a similar physical function of normal intestinal cells *in vitro* [12]. In this study, the capacity of MBP to mitigate the damage induced by DSS and its underlying mechanism on Caco-2 cells were investigated. The results of cell viability and LDH indicated that exposure to MBP did not exert any toxic effects on Caco-2 cells. In published research, excessive production of ROS disrupts cellular defences, leading to oxidative stress and irreversible mitochondrial damage, which are pivotal in the pathogenesis of intestinal inflammation [22]. MBP of 80, 160, 320 μg/mL significantly mitigated the DSS-induced elevation of intracellular ROS levels through enhancing the activity of the antioxidant enzyme SOD. Excessive oxidative stress initiates an inflammatory response, with pro-inflammatory cytokines such as TNF-α and other chemokines playing a significant role in mediating the inflammatory response in Caco-2 cells [19]. Consistent with anticipated outcomes, except for the group treated with 40 μg/mL of MBP, the levels of TNF-α and IL-6 was lower in the groups treated with MBP (80-320 μg/mL), relative to MC group.

Pro-inflammatory cytokines, produced by cells in inflammatory state, induce the expression of a class of membrane-bound proteins, including COX-2, and elevated COX-2 further induces apoptosis, which is involved in a variety of pathophysiological processes [33]. The expression of COX-2 protein in cells after MBP treatment was significantly reduced when compared to the MC group. The most pronounced effect was observed at high doses of MBP, in accord with the outcomes of the cell viability and toxicity assay. These findings suggest that restoration of cellular oxidative stress balance is a key mechanism by which MBP mitigates DSS-induced cytotoxicity.

Excessive oxidative stress can induce DNA damage and trigger apoptosis, a process that is a key target for many bioactive compounds [34-35]. Our results indicate that MBP is involved in programmed cell death and reduces apoptosis in Caco-2 cells following DSS treatment. Specifically, pretreatment with 320 μg/mL of MBP significantly decreased the proportion of cells in G0/G1 phase, bringing it closer to the levels observed in the NC group. This suggested that MBP might restore the normal growth cycle of Caco-2 cells. Caspases, a family of cysteine-containing aspartate-specific proteases, play a critical role in the apoptosis. Among them, Caspase-3 is cleaved and activated to generate Cleaved-caspase-3, which is a key effector of apoptosis [30]. In addition, the Bcl-2 family of proteins, which includes both anti-apoptotic (Bcl-2) and pro-apoptotic proteins (Bax), is crucial during apoptosis. Western Blot experiments revealed that DSS induced activation of

caspase-3 proteins in Caco-2 cells, but this activation was mitigated by MBP pre-treatment. The ratio of cleaved-caspase-3 was significantly reduced, while the ratio of Bcl-2 to Bax protein was significantly increased. In summary, these findings suggest that MBP ameliorated DSS-induced growth cycle arrest and attenuated apoptotic state in Caco-2 cells, potentially through modulation of the Caspase-3/Bcl-2/Bax signalling pathway.

In addition, the expression of TJs protein in Caco-2 cell was assessed to examine the integrity of tight junctions between cells. Tight junction proteins play important role in maintaining the stability and integrity of intestinal barrier. Claudins form the characteristic tight junction strands and create paracellular channels, ZO-1 and occludin regulate epithelial apoptosis and proliferation, facilitate viral entry, and organize specialized epithelial structures [36-37]. The results indicated that 80-320 μg/mL of MBP significantly increased the expression of Claudin protein in DSS-induced Caco-2 cells. However, no significant change was observed in Occludin protein expression. To further investigate the effects of MBP and DSS on intestinal epithelial cell barrier integrity, TEER, fluorescent yellow permeability and TJs protein expression in Caco-2 cell monolayer model was tested. DSS treatment has been shown to damage intestinal cells and increase intestinal permeability [38-39]. Polysaccharide from *Poria cocos* (PCP) improves intestinal barrier function by increasing the expression of Wnt/β-Catenin and Lrp5 proteins, and modulates intestinal barrier function by altering the microbial composition of the gut [40]. Peach gum polysaccharide alleviates pneumonia by restoring the integrity of the intestinal barrier, increasing the production of short-chain fatty acids (SCFAs), reducing the inflammatory response and oxidative stress [41]. *Dendrobium officinale* oligosaccharides modulate the gut microbiota structure and increased the secretion of SCFAs to maintain intestinal homeostasis in colitis mice [42]. In addition, *Artemisia argyi* polysaccharides also increased the content of SCFAs, alleviated intestinal inflammation and intestinal flora dysbiosis in LPS-treated mice by regulating intestinal flora [43].

In this study, DSS treatment induced decreased TEER values, increased monolayer permeability, and reduced expression of three types of TJs proteins (ZO-1, Occludin and Claudin). However, pretreatment with MBP significantly stabilized the TEER value, enhanced intercellular tightness to prevent the permeability of fluorescent yellow, and significantly promoted the expression of TJs protein. Thus, the results suggest that MBP had the potential to ameliorate DSS-induced damage to Caco-2 cell *in vitro* by maintaining barrier integrity and modulating TJ protein expression.

5. Conclusions

In the present study, we demonstrated that DSS has a significant toxic effect on Caco-2 cells, manifested as dysregulated oxidative stress state and cell apoptosis, damaged intestinal barrier function and integrity, the mechanism was revealed as reducing SOD activity and the expression of TJ-related proteins, including ZO-1, occluding and claudin, increasing release of inflammatory factors such as TNF-α and IL-6, as well as increasing the expression of COX-2 protein. MBP exhibited the protection effect on DSS-induced Caco-2 cells by improving the cell viability and alleviating the oxidative stress and inflammatory state induced by DSS. Furthermore, MBP mitigated DSS-induced apoptosis in Caco-2 cells via the Caspase-3/Bcl-2/Bax

pathway and maintained the integrity and stability of Caco-2 monolayer cell through upregulating expression of TJs proteins. Our findings suggest that the protective effects of MBP on DSS-induced damage in human Caco-2 cells may be attributed to its ability of improving intestinal barrier integrity, antioxidant activity and anti-inflammatory effect. This study could improve the understanding about the potential mechanisms of MBP protection against DSS-induced toxic effect on Caco-2 cell, and highlight the potential of MBP as a therapeutic agent for the treatment of ulcerative colitis.

Conflict of interest

The authors declare no conflict of interest.

Acknowledgements

This research was financially supported by the National Key Research and Development Program of China (2023YFF1104001), Natural Science Foundation of Jiangxi Province, China (20232BCD44003).

References

[1] L. W. Peterson, D. Artis, Intestinal epithelial cells: regulators of barrier function and immune homeostasis. Nature Reviews Immunology, 14(3), (2014) 141–153. https://doi.org/ 10.1038/nri3608.

[2] L. Shen, J. R. Turner, Role of epithelial cells in initiation and propagation of intestinal inflammation. Eliminating the static: tight junction dynamics exposed. American Journal of Physiology-Gastrointestinal and Liver Physiology, 290(4) (2006) G577-G582. https://doi.org/10.1152/ajpgi.00439.2005.

[3] C. Le Berre, S. Honap, L. Peyrin-Biroulet, Ulcerative colitis. The Lancet 402(10401) (2023) 571-584.

[4] K. Amandip, G. Paraskevi, Ulcerative colitis: understanding its cellular pathology could provide insights into novel therapies. Journal of Inflammation, 17 (2020), 15. https://doi.org/10.1186/s12950-020-00246-4.

[5] L. Cui, X. Guan, W. Ding, Y. Luo, W. Wang, et al., *Scutellaria baicalensis* Georgi polysaccharide ameliorates DSS-induced ulcerative colitis by improving intestinal barrier function and modulating gut microbiota. International Journal of Biological Macromolecules, 166 (2021) 1035-1045. https://doi.org/10.1016/j.ijbiomac.2020.10.259.

[6] L. Huang, M. Huang, M. Shen, P. Wen, T. Wu, Y. Hong, J. Xie, et al., Sulfated modification enhanced the antioxidant activity of *Mesona chinensis* Benth polysaccharide and its protective effect on cellular oxidative stress. International Journal of Biological Macromolecules, 136 (2019) 1000-1006. https://doi.org/10.1016/j.ijbiomac.2019.06.199.

[7] X. Chen, M. Shen, J. Yang, Q. Yu, Y. Chen, X. Wang, et al., RNA-seq based elucidation of mechanism underlying Mesona chinensis Benth polysaccharide protected H_2O_2-induced oxidative damage in L02 cells. Food Research International, 157 (2022) 111383. https://doi.org/10.1016/j.foodres.2022.111383.

[8] H. Lu, M. Shen, Y. Chen, Q. Yu, T. Chen, J. Xie, Alleviative effects of natural plant polysaccharides against DSS-induced ulcerative colitis via inhibiting inflammation and modulating gut microbiota. Food Research International, 167 (2023) 112630. https://doi.org/ 10.1016/j.foodres.2023.112630.

[9] H. Lu, M. Shen, T. Chen, Y. Yu, Y. Chen, Q. Yu, X. Chen, J. Xie, Mesona chinensis Benth polysaccharides alleviate DSS-induced ulcerative colitis via inhibiting of TLR4/MAPK/NF-κB signaling pathways and modulating intestinal microbiota. Molecular Nutrition & Food Research, 2022, 66, 2200047. https://doi.org/10.1002/mnfr.202200047.

[10] L. Huang, M. Shen, T. Wu, Y. Yu, Q. Yu, Y. Chen, J. Xie, *Mesona chinensis* Benth polysaccharides protect against oxidative stress and immunosuppression in cyclophosphamide-treated mice via MAPKs signal transduction pathways. International Journal of Biological Macromolecules, 152 (2020) 766-774. https://doi.org/10.1016/ j.ijbiomac.2020.02.318.

[11] P. Nimishraj, M. G. Phillip, The Caco-2 Model: Modifications and enhancements to improve efficiency and predictive performance. International Journal of Pharmaceutics, 624 (2022) https://doi.org/10.1016/j.ijpharm.2022.122004.

[12] S. Kamiloglu, E. Capanoglu, C. Grootaert, J. Van Camp, Anthocyanin absorption and metabolism by human intestinal Caco-2 cells -- A review. International Journal of Molecular Sciences, 16(9) (2015) 21555-21574. https://doi.org/10.3390/ijms160921555.

[13] L. Lin, J. Xie, S. Liu, M. Shen, W. Tang, M. Xie, Polysaccharide from *Mesona chinensis*: Extraction optimization, physicochemical characterizations and antioxidant activities. International Journal of Biological Macromolecules, 99(2017), 665-673, https://doi.org/10.1016/j.ijbiomac.2017.03.040.

[14] F. Tao, G. Z. Biao, J. Z. Yu, Z. H. Ning, Isolation and characterization of an acidic polysaccharide from Mesona Blumes gum. Carbohydrate Polymers, 71(2) (2008) 159-169. https://doi.org/10.1016/j.carbpol.2007.05.017.

[15] L. Cai, X. Qin, Z. Xu, Y. Song, H. Jiang, Y. Wu, H. Ruan, J. Chen, Comparison of cytotoxicity evaluation of anticancer drugs between real-time cell analysis and CCK-8 method. ACS Omega Journal, 4 (2019) 12036–12042. https://doi.org/10.1021/acsomega. 9b01142.

[16] Q. Xiang, W. Zhang, Q. Li, J. Zhao, W. Feng, T. Zhao, et al., Investigation of the uptake and transport of polysaccharide from Se-enriched Grifola frondosa in Caco-2 cells model. International Journal of Biological Macromolecules, 158 (2020) 1330-1341. https://doi.org/10.1016/j.ijbiomac.2020.04.160.

[17] P. Artursson, K. Palm, K. Luthman, Caco-2 monolayers in experimental and theoretical predictions of drug transport. Advanced Drug Delivery Reviews, 64 (2012) 280-289. https://doi.org/10.1016/j.addr.2012.09.005.

[18] K. W. Chang, C. Y. Kuo, 6-Gingerol modulates proinflammatory responses in dextran sodium sulfate (DSS)-treated Caco-2 cells and experimental colitis in mice through adenosine monophosphate-activated protein kinase (AMPK) activation. Food & Function, 6(10) (2015) 3334-3341. https://doi.org/10.1039/C5FO00513B.

[19] K. Priti, N. Arvindhan, D U. Pradeep, Analysis of Cell Viability by the Lactate Dehydrogenase Assay. Cold Spring Harb Protoc. 6(2018). https://doi.org/10.1101/pdb.prot095497.

[20] Y. Li, X. Tian, S. Li, L. Chang, P. Sun, Y. Lu, W. Kang, et al., Total polysaccharides of adlay bran (Coix lachryma-jobi L.) improve TNF-α induced epithelial barrier dysfunction in Caco-2 cells via inhibition of the inflammatory response. Food & Function, 10(5) (2019) 2906-2913. https://doi.org/10.1039/C9FO00590K.

[21] V. Marian, L. Dieter, M. Jan, C. Mark, M. Milan, T. Joshua, Free radicals and antioxidants in normal physiological functions and human disease. The International Journal of Biochemistry & Cell Biology, 39(1) (2007) 44-84. https://doi.org/10.1016/j.biocel.2006.07.001.

[22] B. Asima, C. Ranajoy, M. Sankar, C. S. Crowe, Oxidative stress: an essential factor in the pathogenesis of gastrointestinal mucosal diseases. Physiological Reviews, 94(2) (2014) 329-354. https://doi.org/10.1152/physrev.00040.2012.

[23] F. A. de Freitas, D. Levy, A. Zarrouk, G. Lizard, S. P. Bydlowski, Impact of oxysterols on cell death, proliferation, and differentiation induction: Current status. Cells, 10(9) (2021) 2301. https://doi.org/10.3390/cells10092301.

[24] G. Manda, M. T. Nechifor, T. M. Neagu, Reactive oxygen species, cancer and anti-cancer therapies. Current Chemical Biology, 3(1) (2009) 22-46. See discussions, stats, and author profiles for this publication at: https://www.researchgate.net/publication/228698975.

[25] L. Wang, X. Li, B. Wang, The cytotoxicity activity of Hohenbuehelia serotina polyphenols on HeLa cells via induction of cell apoptosis and cell cycle arrest. Food and Chemical Toxicology, 124 (2019) 239-248. https://doi.org/10.1016/j.fct.2018.12.001.

[26] Y. Araki, K. I. Mukaisyo, H. Sugihara, Y. Fujiyama, T. Hattori, Increased apoptosis and decreased proliferation of colonic epithelium in dextran sulfate sodium-induced colitis in mice. Oncology Reports, 24(4) (2010) 869-874. https://doi.org/10.1023/A:1015931128583.

[27] Y. Chen, J. Shin, H. Wei, C. Lin, L. Yu, W. Liao, C. Chu, et al., Prevention of dextran sulfate sodium-induced mouse colitis by the fungal protein Ling Zhi-8 via promoting the barrier function of intestinal epithelial cells. Food & Function, 12(4) (2021) 1639-1650. https://doi.org/10.1039/D0FO02604B.

[28] M. Birendra, J. Rajesh, Oxidative Stress in the Poultry Gut: Potential Challenges and Interventions. Frontiers in Veterinary Science, 6(2019). https://doi.org/10.3389/fvets.2019.00060.

[29] M. C. Daniel, G. Arash, Contribution of the Intestinal Microbiome and Gut Barrier to Hepatic Disorders. Gastroenterology, 159(3) (2020), Pages 849-863. https://doi.org/10.1053/j.gastro.2020.04.077.

[30] M. Jin, Y. Wang, M. Huang, Z. Lu, Y. Wang, Sulphation can enhance the antioxidant activity of polysaccharides produced by Enterobacter cloacae Z0206. Carbohydrate Polymers, 99 (2014) 624-629. https://doi.org/10.1016/j.carbpol.2013.08.072.

[31] L. Xie, M. Shen, P. Wen, Y. Hong, X. Liu, J. Xie, Preparation, characterization, antioxidant activity and protective effect against cellular oxidative stress of phosphorylated polysaccharide from Cyclocarya paliurus. Food and Chemical Toxicology, 145 (2020) 111754. https://doi.org/10.1016/j.ijbiomac.2018.08.024.

[32] Y.-S. Kim, C.-B. Ahn, J.-Y. Je, Anti-inflammatory action of high molecular weight Mytilus edulis hydrolysates fraction in LPS-induced RAW264.7 macrophage via NF-κB and MAPK pathways. Food Chemistry, 202 (2016) 9-14. https://doi.org/10.1016/ j.foodchem.2016.01.114.

[33] S. J. Desai, B. Prickril, A. Rasooly, Mechanisms of phytonutrient modulation of cyclooxygenase-2 (COX-2) and inflammation related to cancer. Nutrition and Cancer, 70(3) (2018) 350-375. https://doi.org/10.1080/01635581.2018.1446091.

[34] S. Zaman, R. Wang, V. Gandhi, Targeting the apoptosis pathway in hematologic malignancies. Leuk Lymphoma, 55(9) (2014) 1980-1992. https://doi.org/10.1016/j.canlet. 2011.06.016.

[35] L. Zhao, X. Wang, X. L. Zhang, Q. F. Xie, Purification and identification of anti-inflammatory peptides derived from simulated gastrointestinal digests of velvet antler protein (Cervus elaphus Linnaeus). Journal of Food and Drug Analysis, 24(2) (2016) 376-384. https://doi.org/10.1016/j.jfda.2015.10.003.

[36] W. T. Kuo, M. A. Odenwald, J. R. Turner, L. Zuo, Tight junction proteins occludin and ZO-1 as regulators of epithelial proliferation and survival. Annals of the New York Academy of Sciences, 1514 (2022) 21–33. https://doi.org/10.1111/nyas.14798.

[37] H. Park, D. Kweon, J. Kim, Molecular weight-dependent hyaluronic acid permeability and tight junction modulation in human buccal TR146 cell monolayers. International Journal of Biological Macromolecules. 227 (2023) 182–192. https://doi.org/10.1016/j.ijbiomac.2022. 12.106.

[38] X. Chen, W. Xiao, M. Shen, Q. Yu, Y. Chen, J. Yang, J. Xie, Changes in polysaccharides structure and bioactivity during *Mesona chinensis* Benth storage. Food Science, 5 (2022) 392-400. https://doi.org/10.1016/j.crfs.2022.01.024.

[39] C. Wang, J. Bai, B. Wang, L. Yu, F. Tian, J. Zhao, et al., Stachyose modulates gut microbiota and alleviates dextran sulfate sodium-induced acute colitis in mice. Food Science and Human Wellness, 12(6) (2020) 2211-2220. https://doi.org/10.1016/j.fshw.2023.03.041.

[40] Y. Duan, J. Huang, M. Sun, Y. Jiang, S. Wang, L. Wang, et al, Poria cocos polysaccharide improves intestinal barrier function and maintains intestinal homeostasis in mice. International Journal of Biological Macromolecules, 249(2023)125953. https://doi.org/10.1016/j.ijbiomac.2023.125953.

[41] S. Li, G. Li, D. Liu, M. Li, H. Liu, W. Zhu, K. Wang, X. Ren, Peach gum polysaccharide protects intestinal barrier function, reduces inflammation and oxidative stress, and alleviates pulmonary inflammation induced by *Enterococcus faecium E745*, Journal of Functional Foods, 115(2024), 106098. https://doi.org/10.1016/j.jff.2024.106098.

[42] D. Shi, P. Wang, L. Xu, H. Zhu, W. Zhang, Q. Wu, T. Bu, B. Tian, P. Sun, M. Cai, Potential of *Dendrobium officinale* oligosaccharides to alleviate chronic colitis by modulating inflammation and gut microbiota, Food & Medicine Homology, 2025, 2: 9420077. https://doi.org/10.26599/ FMH.2025.9420077.

[43] E. Ning, C. Sun, X. Wang, L. Chen, F. Li, Li. Zhang, L. Wang, Y. Ma, J. Zhu, et al., *Artemisia argyi* polysaccharide alleviates intestinal inflammation and intestinal flora dysbiosis in lipopolysaccharide-treated mice, Food & Medicine Homology, 2024, 1: 9420008. https://doi.org/ 10.26599/FMH.2024.9420008.